Free Radicals and Antioxidants., 2023; 13(2):74-85.
https://www.antiox.org

Original Article

Anti-Parkinson Potential of Indian *Ocimum* species in Relation to Active Components as Revealed Using Metabolites Profiling, *in vitro* and *in silico* Enzyme Inhibition Studies

Sreerupa Sarkar[1], Jhelam Chatterjee[1], Aditi Gangopadhyay[2], Mohammed Sheashea[3], Mohamed A. Farag[4], Achintya Saha[2], Susmita Das[1], Bratati De[1,*]

[1]Department of Botany, Phytochemistry and Pharmacognosy Research Laboratory, University of Calcutta, Kolkata, West Bengal, INDIA.
[2]Department of Chemical Technology, Drug Design and Cheminformatics Laboratory, University of Calcutta, Kolkata, West Bengal, INDIA.
[3]Department of Aromatic and Medicinal Plants, Desert Research Center, Cairo, EGYPT.
[4]Department of Pharmacognosy, Faculty of Pharmacy, Cairo University, Cairo, EGYPT.

ABSTRACT

Background: Parkinson's Disease (PD) is a debilitating neurodegenerative disease suffered by elderly population worldwide. There are different treatment options for its symptomatic relief including the use of inhibitors of monoamine oxidase-B, acetylcholinesterase enzymes and L-DOPA though with certain side effects. **Materials and Methods:** To identify new resources of natural products with potential effects to treat PD, several Indian *Ocimum* species, e.g., *O. tenuiflorum* (green), *O. tenuiflorum* (purple), *O. basilicum, O. americanum, O. kilimandscharicum,* and *O. gratissimum* were screened. Activities of the extracts were studied against monoamine Oxidase-B (MAO-B), and acetylcholinesterase (AChE). Identification of active components present in these extracts was determined using GC-MS and LC-MS metabolites profiling. Further, activity of identified phenolics was measured by docking score against MAO-B and AChE. **Results:** All extracts and several phenolics showed potential inhibition of these two PD related enzymes based on *in vitro* and *in silico*, respectively. Ellagic acid-di-methyl ether-O-glucoside, rosmarinic acid, and luteolin-5-glucuronide were identified as top scoring hits against both AChE and MAO-B from molecular docking studies. L-DOPA was also detected in all the species of *Ocimum*. **Conclusion:** IC_{50} values against both enzymes and L-DOPA levels detected in *O. tenuiflorum* (green), *O. basilicum,* and *O. americanum* pose them as potential nutraceuticals for PD treatment.

Keywords: Parkinson's Disease, *Ocimum species*, monoamine oxidase-B, acetylcholinesterase, L-DOPA.

Correspondence:
Dr. Bratati De
Department of Botany, Phytochemistry and Pharmacognosy Research Laboratory, University of Calcutta, Kolkata, West Bengal, INDIA.
Email: bratatide@hotmail.com

Received: 17-11-2023;
Revised: 02-12-2023;
Accepted: 22-01-2024.

INTRODUCTION

The age-related neurodegenerative diseases of the central nervous system include mostly Parkinson's Disease (PD), Alzheimer's Disease (AD) and Huntington's Disease (HD). PD, a progressive debilitating disease, is the second most common oxidative stress associated neurodegenerative disease next to AD. Current oral PD treatment options for providing symptomatic relief include mostly the use of a dopamine precursor (levodopa or L-DOPA), dopamine agonists (apomorphine, bromocriptine etc.), and inhibitors of Monoamine Oxidase-B (MAO-B). MAO-B catalyzes dopamine catabolism. MAO-B inhibitors (selegilline, rasagilline) are used therapeutically to prevent against its catabolism thus increasing dopamine level inside the brain.[1,2] Activated MAOB leads to cognitive dysfunction, destruction of cholinergic neurons, and contributes to the formation of amyloid plaques.[2] Anticholinergics (benzatropine, trihexiphenidyl) modulate the activity of acetylcholine.[1] Acetylcholinesterase inhibitors are well established treatment for PD dementia related gait disturbance, and imbalance in PD.[3] Certain MAO-B inhibitors are used therapeutically for the symptomatic treatment of PD,[4] either alone or in combination with L-DOPA. However, MAO-B inhibitors have some adverse effects like depression, hallucinations, confusion etc.[5] L-DOPA, a precursor of dopamine is a therapeutic drug used to decrease motor symptoms of PD, though likewise suffering from certain side effects like dyskinesia.[6] Efforts for the search of other safe medicine from natural products for PD management appears rewarding to overcome these problems.

DOI: 10.5530/fra.2023.2.13

Copyright Information :
Copyright Author (s) 2023 Distributed under Creative Commons CC-BY 4.0

Publishing Partner : EManuscript Tech. [www.emanuscript.in]

Different species of *Ocimum* are used in culinary, cosmetics, medicinal and fragrance industries.[7] Examples of major *Ocimum* species include *O. sanctum, O. tenuiflorum, O. basilicum, O. americanum, O. minimum, O. africanum, O. gratissimum, O. kilimandscharicum, O. canum*, etc. that are grown in different parts of Asia, Africa, South America, and Europe. *Ocimum* species have been used to treat different ailments in Ayurveda, and the traditional systems of medicine in China, Africa, etc.[7] For example, *O. sanctum* has been used for thousands of years in Ayurveda for the treatment of different ailments such as common cold, headaches, stomach disorders, inflammation, heart disease, malaria etc.[8] *O. basilicum* is likewise used in Indian traditional system of medicine to treat different health problems.[6]

The main goal of the present study was to assess inhibition effects of extracts of Indian *Ocimum* species against MAO-B and AChE, two enzymes implicated in PD progression, and in relation to their metabolite fingerprint as determined using gas chromatography and liquid chromatography coupled to mass spectrometry. Further, *in silico* docking was performed to provide insight on the inhibition capacity of the main chemicals identified in active extracts of the *Ocimum* species against MAO-B and AChE for identification of binding sites and future development as drugs.

MATERIALS AND METHODS

Plant Collection

Leaves of five different *Ocimum* species belonging to Lamiaceae family were collected during the rainy season (June-August). The green variety of *O. tenuiflorum* L. synonym *O. sanctum* L. (Accession No. 20102), purple variety of *O. tenuiflorum* L. (Accession No. 20104), *O. americanum* L. (Accession No. 20106), *O. kilimandscharicum* Guerke (Accession No. 20101), and *O. gratissimum* L (Accession No. 20105) were collected from the medicinal plant garden of Narendrapur Ramakrishna Mission, Kolkata. *O. basilicum* L. (Accession No. 20103) was collected from the Agri Horticulture Society of India, Kolkata, West Bengal, India. Taxonomic identification of the species was done through the Acceession No., Botanical Survey of India, Howrah, West Bengal, India. These specimens were deposited in the Calcutta University Herbarium, Kolkata, West Bengal, India.

Chemicals

Ribitol, methoxyamine hydrochloride, N-methyl-N-Trimethylsilyltrifluoroacetamide (MSTFA) with 1% Trimethylchlorosilane (TMCS), methyl octanoate (C8), methyl decanoate (C10), methyl laurate (C12), myristic acid methyl ester (C14), methyl palmitate (C16), stearic acid methyl ester (C18), methyl arachidate (C20), methyl behenate (C22), methyl tetracosanoate (C24), methyl hexacosanoate (C26), pargyline hydrochloride, kynumarine dihydrobromide, acetylcholinesterase from *Electrophorus electricus*, human MAO-B (recombinant, expressed in baculovirus infected BTI insect cells) were obtained from Sigma-Aldrich (St. Louis, MO, USA). Sodium dihydrogen phosphate dehydrate crystal, di-sodium hydrogen phosphate anhydrous, potassium dihyrogen phosphate, di-potassium hydrogen phosphate anhydrous, potassium chloride, Folin-Ciocalteau reagent, sodium hydroxide, sodium carbonate, dimethyl sulfoxide, and pyridine were purchased from Merck Specialities Private Limited. Acetylthiocholine iodide, 5,5, dithiobis (2-nitrobenzoic acid) or DTNB were purchased from Sisco Research Laboratories Pvt. Ltd., (SRL); 3,4 dihydroxy L-phenylalanine (L-DOPA) from Hi Media Laboratories Pvt. Ltd., All the other chemicals and reagents used for the preparation of the samples were of analytical grade, and all the solvents used for GC/MS, LC-MS were of HPLC grade.

Preparation of crude extracts

Leaves of each species were ground using liquid nitrogen. The powder (about 400-500 g) was extracted, modifying the method of Sultana *et al.*,[9] with 70% methanol (1-1.2 L) at 60-70°C for 3 hr in a boiling water bath with occasional stirring. After cooling, extracts were centrifuged at 10,000 rpm for 20 min. The supernatants were pooled and then evaporated to dryness at 70°C using rotary evaporator. Dried extracts were kept at -20°C till further experiments.

Monoamine Oxidase-B inhibition assay

Monoamine Oxidase-B (MAO-B) enzyme inhibition activity of *Ocimum* extracts were assayed *in vitro* using human MAO-B (recombinant, expressed in baculovirus infected BTI insect cells) following Cloete *et al.*[10] The whole reaction was performed in an alkaline medium. The reaction mixture was composed of potassium phosphate buffer (pH 7.4, 100 mM, made isotonic with KCl), kynuramine dihydrobromide (50 µM) as a substrate, MAO-B (0.015 mg protein/mL) from stock solution (2.5 mg protein/mL), and 8.5 µL of different concentrations (0.1 mg/mL to 1.5 mg/mL) of plant extracts (dissolved in DMSO). Kynuramine dihydrobromide and MAO-B were dissolved in potassium phosphate buffer. After the addition of enzyme (MAO-B), reaction mixture was incubated at 37°C for 20 min. Reaction was terminated with the addition of 2N NaOH solution till a final volume of the reaction mixture of 200 µL. 4-Hyroxyquinoline generated was measured using fluorescence spectrophotometry [excitation wavelength (λ_{ex}=310 nm); emission wavelength (λ_{em} =400 nm)] using a 96 well plates microplate reader. Regression equations were prepared from the concentrations of the extracts and percentage inhibition of MAO-B activity. IC_{50} values (concentration of sample required for 50% inhibition of enzyme activity) were calculated from these regression equations. Each experiment was repeated in triplicates.

Acetylcholinesterase inhibition assay

Acetylcholinesterase (AChE) enzyme inhibition activity of *Ocimum* extracts was assayed *in vitro* following Ellman *et*

al.[11] using AChE from electric eel. The reaction mixture was composed of 70% methanol solution of extract (0.01 mL), 0.02 mL AChE (19.93 unit/mL buffer, pH 8) and 1 mL buffer. The reaction was initiated by the addition of 0.02 mL substrate acetylthiocholine iodide (0.6 mM) and 0.01 mL of 0.5 mM 5,5,Dithiobis (2-Nitrobenzoic Acid) (DTNB) solution. DTNB acted as color developer when it reacts with thiocholine (final product). The reaction mixture was incubated at 37°C for 20 min. The optical density was measured at 412 nm immediately using UV-vis spectrophotometer. Regression equations were derived from concentrations of extracts (0.1 mg/mL to 1.5 mg/mL) and percentage inhibition of AChE activity, with IC_{50} values calculated from regression equation. Each experiment was repeated 4 times.

Ultra-Performance Liquid Chromatography/Mass Spectroscopy (UPLC/MS) analysis

The analysis of UPLC-ESI-MS/MS in both negative and positive mode were performed on Xevo TQD triple quadrupole instrument Waters Corporation, Milford, MA01757, USA, mass spectrometer. Sample was (100 µg/mL) prepared by using methanol HPLC analytical grade which was filtered through a disc filter (PTFE, 0.2 µm). The injection volume was 10 µL introduced into reverse phase C18 column (ACQUITY UPLC-BEH C18 1.7µm particle size, 2.1x50 mm column). Gradient elution was done at a flow rate of 1.5 mL/min using mobile phase composed of two eluents: eluent A (acetonitrile) and eluent B (methanol with 0.5 mM ammonium acetate). The gradient flow was carried out as follows: 95% A, 1-16; 5% A, 16-18; %5 A, 18-20; 95% A, 20-22. Parameters for analysis were source temperature 150°C, cone voltage 43.7 eV, capillary voltage 1.73 kV, desolvation temperature 348°C, cone gas flow 30 L/hr and desolvation gas flow 944 l/h. Mass spectra were detected in the ESI positive and negative modes scanning between m/z 100-900. The peaks, spectra and relative peak areas were processed using Masslynx 4.1 software and identification was based on molecular weight, fragmentation pattern and reported data from literature.[12]

Gas Chromatography/Mass Spectrometry (GC/MS) analysis

Crude extract (10 mg) prepared from each *Ocimum* species was dissolved in methanol: water (1:1) solution. Ribitol (20 µL of 0.2 mg/mL aqueous solution) was added as an internal standard in each solution. 100 µL of each sample was distributed into eppendorf tubes and evaporated to dryness. The residue was re-dissolved in 5 µL of methoxyamine hydrochloride (20 mg/mL prepared in Pyridine) and subsequently shaken for 90 min at 30°C. The metabolites were derivatized[13] by 45 µL of N-Methyl-N-Trimethylsilyltrifluoroacetamide (MSTFA) with 1% Trimethylchlorosilane (TMCS). Fatty Acid Methyl Esters (FAME) markers (1 µL) [a mixture of internal Retention Index (RI) markers prepared using fatty acid methyl esters of C_8, C_{10}, C_{12}, C_{14}, C_{16}, C_{18}, C_{20}, C_{22}, C_{24}, and C_{26} linear chain length, dissolved in chloroform (HPLC) at two different concentrations such as 0.8 mg/mL and 0.4 mg/mL for C_8-C_{16} and C_{18}-C_{26} respectively] was added into the mixture. GC-MS analysis was carried out by the method of Das and De.[14] HP-5MS capillary column of 30 m length, 0.25 mm narrow bore diameter and 0.25 µm inner film (Agilent J and W; GC Columns (USA) was used for GC-MS analysis. Oven temperature was programmed as such: oven ramp 60°C (1 min hold) to 325°C at 10°C/min; 10 min hold before cool-down and 37.5 min run time. 250°C temperature was set for injector, 290°C and 230°C temperature were set for the MS transfer line and for the ion source respectively. Helium was used as the carrier gas at a constant flow rate of 0.723 mL/min (carrier linear velocity 31.141 cm/sec). Sample (1 µL) was injected onto the GC column using a split ratio of 1:5. Automated Mass spectral Deconvolution and Identification System (AMDIS) was used for the analysis of chromatographic peaks and mass spectra. The mass spectral fragmentation pattern, Retention Times (RT) and Retention Indices (RI) were compared with entries in Fiehn GC-MS Metabolomics Library (Agilent GC-MS Metabolomics RTL Library, 2008). Several peaks were confirmed using authentic whenever available. Normalized relative response ratios were obtained by dividing peak areas to that of internal standard ribitol.

Determination of total phenolics

Total phenolic content was measured using Folin-Ciocalteau reagent.[15] Folin-Ciocalteau (0.5 mL) and 3 mL of each plant extract were mixed in an eppendorf tube. Sodium carbonate solution (2 mL of 20% aqueous solution) was added immediately after 3 min of incubation at room temperature. Later the mixture was placed in a boiling water bath for 1 min. The total reaction mixture was allowed to cool down. After that optical density of the reaction mixture was measured against blank solution. Total phenol content was measured as mg/mg gallic acid equivalent.

Ligand and receptor structure docking assay

The 2D structures of 44 compounds of *Ocimum* sp. were retrieved from PubChem in SDF format. The 3D structures of the compounds were generated with LigPrep, Schrödinger, using the OPLS4 force field.[16] All possible states of the ligands were generated at pH values of 7.0±2.0, and the compounds were desalted during ligand preparation. The specific chirality was retained and a maximum of 32 structures were generated per ligand. The ADMET properties of the compounds, including the Blood-Brain Barrier (BBB) score, CACO-2 permeability, LD_{50}, plasma half-life, P-Gp substrate activity, P-Gp inhibition, and potential reactive groups were predicted using ICM-Pro.

The structures of AChE and MAO-B were retrieved from the Protein Data Bank (PDB) (PDB IDs: 4EY6 and 1GOS, respectively), were bound to the inhibitors, galantamine and N-[(E)-methyl](phenyl)-N-[(E)-2-propenylidene] methanaminium, respectively.[17-19] The missing residues and

side chains were filled in using Modeller version 10.1,[20] and the structures were prepared with the protein preparation wizard suite in Maestro, Schrödinger, prior to docking.[21] The optimum protonation states of Asn, Gln, His, and hydroxyl groups were generated at pH of 7.0 using PROPKA.[22,23] The water molecules that were 3.0 Å beyond the hetero groups were removed. The structures were finally subjected to restrained minimisation using the OPLS4 force field, in which the heavy atoms were restrained.[16]

Grid preparation, ligand docking, and hit selection

The binding sites of the inhibitors, galantamine and N-[(E)-methyl](phenyl)-N-[(E)-2-propenylidene] methanaminium, bound to AChE and MAO-B, respectively, were considered for grid preparation. The dimensions of the grid were 22 Å, 22 Å, and 22 Å for AChE and 20 Å, 20 Å, and 20 Å for MAO-B, along the x-, y-, and z-axes, respectively. The docking protocol was validated by re-docking the bound inhibitors to the binding site of the receptors. Hit selection was achieved by comparing docking scores of the ligands with those of the reported standards, galantamine and pargyline, of AChE and MAO-B, respectively. The reported standards and ligands of metabolites identified in *Ocimum* species were docked to the binding site of AChE and MAO-B with the Glide Extra Precision (XP) mode.[24,25] The ligand-receptor interactions were determined with Maestro, Schrodinger.[26]

Statistical analyses

In vitro assays were repeated 4 times. IC_{50} values were calculated from regression equations. Data are presented as meanstandard deviation/standard error.

RESULTS

Enzyme inhibition assay

Leaf extracts of all *Ocimum* species inhibited MAO-B in a dose dependent manner. Based on IC_{50} values, highest activity was observed in green variety of *O. tenuiflorum* followed by *O. basilicum* versus lowest effect observed in *O. gratissimum* (Figure 1). Results were compared with the activity of pargyline hydrochloride (IC_{50} value=0.000093 mg/ml ± 0.00 mg/ml), a MAO-B inhibitor.[27] The activities of each extract were found significantly lower than that of pargyline hydrochloride.

Likewise, the extracts of all species of *Ocimum* inhibited AChE in a dose dependent manner. AChE is another target of PD management. Based on IC_{50} values (Figure 2), *O. basilicum* showed the strongest inhibition of AChE followed by *O. americanum* and green variety of *O. tenuiflorum*. In contrast, *O. gratissimum* showed the lowest inhibitory activity. Galantamine, the standard drug as reported previously,[28] exhibited IC_{50} at 0.008 mg/mL. Activities of *Ocimum* leaf extracts were significantly lower than that of galantamine. To reveal whether acetylcholinesterase inhibitory activity was correlated with total phenol content, regression analysis was employed showing r=-0.4983, (df15). IC_{50} values were found to be inversely related to total phenolics. In contrast, MAO-B activity showed no obvious correlation with total phenolic content. AChE inhibitory activity has been previously reported for *O. basilicum, O. africanum, O. americanum*, and *O. minimum* grown in Egypt,[12] and extend herein to include 4 new species reported to exhibit AChE inhibitory properties such as *O. tenuiflorum* (green), *O. tenuiflorum* (purple), *O. kilimandscharicum,* and *O. gratissimum*.

Metabolites profiling in *Ocimum* species using GC-MS

To aid identification of metabolites composition in these *Ocimum* leaves to mediate for its effects, metabolites profiling was attempted using GC-MS. Major classes included organic acids, amino acids, fatty acids, and sugars, in addition to phenolics.[29] Phenolics identified in different species are shown in Table 1.

Additionally, all species of *Ocimum* contained the non-protein amino acid L-DOPA as revealed using GC-MS (Table 1). The relative response ratios of L-DOPA levels are presented in Figure 3, detected at highest amount in *O. americanum*, followed by *O. basilicum* and *O. tenuiflorum* (green variety). In contrast, the lowest L-Dopa content was observed in *O. gratissimum* (Figure 3).

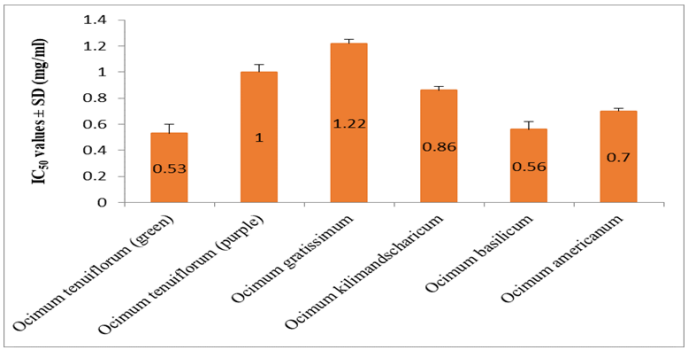

Figure 1: MAO-B inhibitory activities.

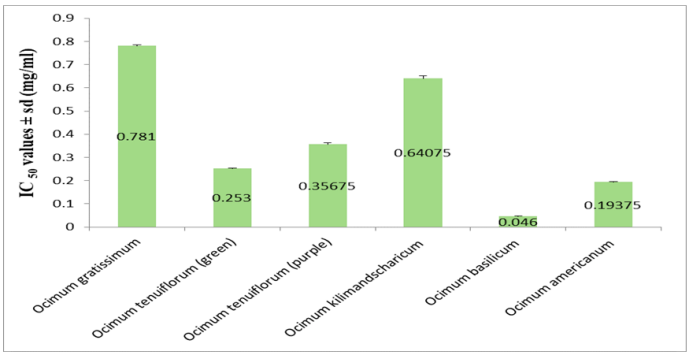

Figure 2: AChE inhibitory activities.

Secondary metabolites profiling in *Ocimum* species using UPLC/MS

Compared to GC/MS metabolites profiling to provide insight on primary metabolites, UPLC/MS is more suited for secondary metabolites that are likely to account for leaf biological effects.[30] Metabolites profiling of 6 *Ocimum* species revealed the identification of 30 compounds including 15 flavonoids, 9 phenolic acids and derivatives, two organic acids, two fatty acids, tannin and diterpene. Metabolites were identified by comparing their MS and MS2 data with available literature as presented in Table 2 alongside their retention time, molecular formulas, and fragmentation pattern. 18 Metabolites were identified in negative mode while 13 metabolites were detected in positive mode attributed to the improved sensitivity level of negative ion mode. Details of metabolites identification shall be described in the next subsections.

Identification of flavonoids

Peak 1, identified as epicatechin with $[M+H]^+$ at *m/z* 291, yielded fragment ion at *m/z* 244 as loss of 47 Da. Peak 7 was identified as isorhamnetin with $[M-H]^-$ at m/z 315 and further fragment 245 supporting its identification.[31] Peak 9 was identified as isorhamnetin-3-(2'' acetylglucoside) with $[M-H]^-$ at *m/z* 519. The fragmentation pattern exhibited the presence of abundant fragment 315 due to loss of acetyl moiety. Another flavonol was identified in peak 11 as kaempferol with $[M-H]^-$ at *m/z* 285 and fragment ion at 153 owing to the consecutive loss of CO.[14] Peak 12 was identified as luteolin-*O*-glucuronide with $[M+H]^+$ at *m/z* 463. The precursor ion yielded fragment ion *m/z* 287 related to aglycone unit with loss of sugar moiety. Peak 12 was identified as luteolin 5-glucuronide with $[M+H]^+$ at *m/z* 461. Peak 14 was identified as apigenin-*O*-glucuronide with $[M+H]^+$ at *m/z* 447 and yielding fragment ion *m/z* 270 with chemical formula $C_{15}H_{10}O_5$. Peak 17 was identified as quercetin with $[M+H]^+$ at *m/z* 302. The fragmentation pattern produced by fragment ion 286 owing to loss of methyl radical and 258 for subsequent loss of CO.[32]

Peak 20 was identified as isothymusin with $[M+H]^+$ at *m/z* 331. The fragmentation pattern revealed the presence of *m/z* 298 [M+H-32] corresponding to the loss of methyl radical and water molecule.[18] Peak 21 was identified as cirsiliol with $[M+H]^+$ at *m/z* 331 yielding fragment ion *m/z* 286 [M+H-45]. Peak 22 was identified as dihydroxy dimethoxyflavone with $[M-H]^-$ at *m/z* 313 and further fragment ion *m/z* 298 owing to loss of methyl group.[12] Peak 23 (cirsimaritin) with chemical formula showed $[M+H]^+$ ion at *m/z* 315 revealing its fragment ion *m/z* 279 [M+H-36]. Peak 24 was identified as nevadensin with $[M+H]^+$ at *m/z* 345 and confirmed based on fragments appearing at *m/z* 299 [M+H-46] and 177 [M+H-168]. Peak 29 was identified as apigenin-*O*-dimethyl ester at retention time 15.304 min with $[M+H]^+$ at *m/z* 299 and showing loss of methyl radical and CO.[32]

Identification of phenolics acids

Peak 2, identified as caffeic acid-*O*- hexoside with $[M-H]^-$ at *m/z* 341 showed loss of glucose residue to yield T fragment ion *m/z* 179 ($C_6H_{10}O_5$).[12] Peak 4 was identified as sinapic acid with $[M+H]^+$ at m/z 225 and further fragments ion at *m/z* 169 [M+H-56] and 154 [M+H-71] characteristic of sinapic acid. Fragment ion 179 manifested the identification of salvialinic acid with $[M-H]^-$ at *m/z* 197 and the fragmentation pattern was attributed to loss of water. Peak 10 was identified as caffeic acid with $[M-H]^-$ at

Table 1: Some of the metabolites identified GC-MS.

Compound name	Rt sample	Rt Library	RI sample	RI Library	m/z	1	2	3	4	5	6
Cinnamic acid*	13.381	13.562	1220	1227.1	205	-	-	-	-	+	-
O-Acetylsalicylic acid*	12.786	13.044	1171.5	1179.3	267	+	+	+	+	+	+
Pyrogallol	13.156	13.456	1201.3	1217.8	239	+	+	+	+		+
Benzene-1,2,4-triol	13.943	14.164	1259.2	1278.27	342	+	-	-	-	+	+
4-Hydroxybenzoic acid*	14.205	14.505	1284.1	1305.2	267	+	+	+	+	+	+
4-Hydroxy-3-methoxybenzoic acid*	15.734	15.989	1418.8	1438.7	297	-	+	-	-	+	+
Shikimic acid	16.211	16.433	1460.2	1483.6	204	+	+	+	+	+	+
Quinic acid*	16.914	17.076	1518.7	1539.2	345	+	+	+	+	+	+
Gallic acid*	17.634	18.012	1579	1630.39	458	-	-	+	+	-	-
Ferulic acid*	18.974	19.312	1692.6	1711.91	338	-	+	+	+	-	-
Caffeic acid*	19.301	19.755	1720.3	1807.7	396	+	+	+	+	+	+
Arbutin	23.219	23.393	2244.8	2045	254	-	-	+	-	-	-
L-Dopa*	18.742	19.089	689.2	732.9	267	+	+	+	+	+	+

1 stands for *O. tenuiflorum* (green variety), 2 for *O. tenuiflorum* (purple variety), 3 for *O. gratissimum*, 4 for *O. basilicum*, 5 for *O. kilimandscharicum* and 6 for *O. americanum*. *Metabolites also identified by matching the spectral characters with that of authentic compounds.

m/z 179. The fragmentation pattern attributed to fragment ion 151 [M-H-28] due to the loss of CO. Peak 15 was identified as rosmarinic acid with $[M-H]^-$ at *m/z* 359. Peak 15 was identified by rosmarinic acid with $[M-H]^-$ at *m/z* 359. Fragment ion 341 was characterized by loss of H_2O from rosmarinic acid. Peak 16 was identified as ferulic acid with $[M-H]^-$ at *m/z* 193. Fragmentation pattern was achieved through four fragment ions: 181 [M-H-12], 173 [M-H-20], 167 [M-H-26] and 153 [M-H-40]. Peak 26 was identified as 4-sinapoyl-*O*-caffeoyl quinic acid with $[M-H]^-$ at *m/z* 559 ($C_{27}H_{27}O_{13}^-$) and its fragment was obtained at *m/z* 381 [M-H-178]. Peaks 28 and 30 were identified as feruloyl tartaric acid and caftaric acid, respectively. The generated fragment ions were 310 [M-H-15] and 295 [M-H-16], respectively.

Identification of fatty and organic acids

Peak 18 was identified as trihydroxy-octadecadiendic acid with $[M-H]^-$ at m/z 327 and its fragment was obtained at *m/z* 313 [M-H-14].

Peak 3 and peak 8 were identified as isocitric acid and hydroxyjasmonic acid hexoside with $[M-H]^-$ at *m/z* 191 and 387, respectively. Fragment ions were attributed to 166 [M-H-25] and 207 resembling aglycone fragment of hydroxyl jasmonic acid.[12]

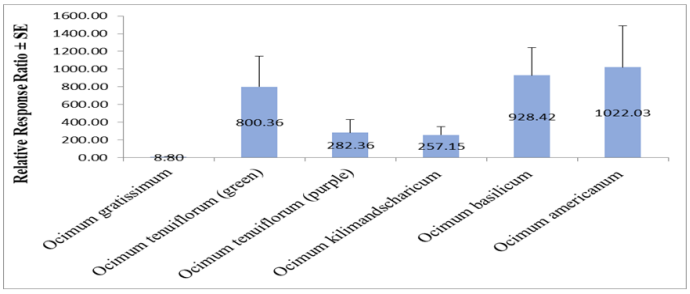

Figure 3: Comparison of content of L-DOPA among six different *Ocimum* species.

Docking of phenolic metabolites of *Ocimum* species to AChE and MAO-B

The activities of the phenolic compounds identified from different *Ocimum* species were studied to AChE and MAO-B by molecular docking. The docking protocol was validated by re-docking with inhibitors, galantamine and N-[(E)-methyl](phenyl)-N-[(E)-2-propenylidene]methanaminium, bound to AChE and MAO-B, respectively. The RMSD values between the crystal pose and docked pose of the bound inhibitors generated with Glide XP were 1.352 Å and 1.409 Å for AChE and MAO-B, respectively, indicating good correlation between the docked and crystal poses. The Glide XP docking scores of the standard reported inhibitors of AChE and MAO-B (galantamine and pargyline, respectively) were -6.925 and -5.586, respectively (Table 3). The compounds with docking scores better (lower) than the reported standards were selected as hits. A total of 27 hits were identified against AChE by comparison of the docking scores with the standard (galantamine), while all compounds of *Ocimum* sp. performed better than the standard inhibitor, pargyline, in terms of the Glide XP score (Table 3). The docking scores of the hits identified against AChE and MAO-B are provided in Table 3.

Ligand-receptor interaction analysis revealed that the hits identified against AChE formed pi-pi interactions with Trp627, Trp827, Tyr878, and His988, implying that these residues were important for ligand binding. The findings also revealed that Ser744 of AChE was the primarily involved in the formation of ligand-receptor hydrogen bonds (Figure 4). Analysis of the ligand-receptor interactions of MAO-B revealed that the ligand-receptor hydrogen bonds were primarily mediated via Ser559, Tyr560, and Gln706 (Figure 5).

ADMET screening

The ADMET properties of the compounds were determined using ICM Pro. The drug-likeliness of the compounds were determined based on Lipinski's rule of five and Veber's rules. Compounds with molHERG scores >0.5 are potential HERG

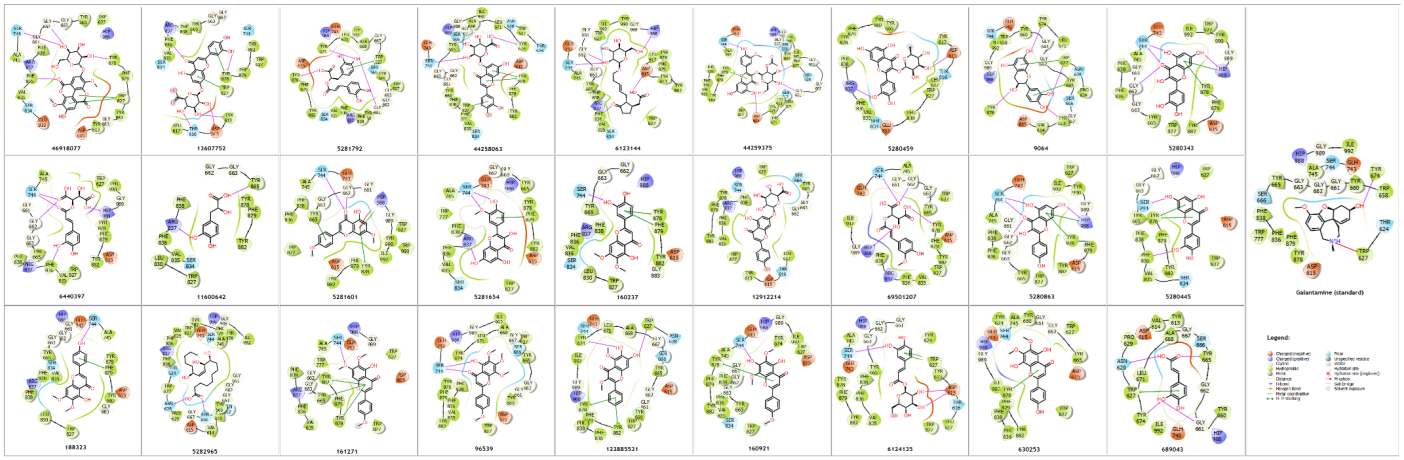

Figure 4: Interactions of the hits identified against AChE and the standard inhibitor, galantamine.

Table 2: Metabolites identified by UPLC/MS.

No.	Rt	Compound name	Chemical formula	M+	M-	Fragments	*1*	*2*	*3*	*4*	*5*	*6*	Chemical class
1	1.208	Epicatechin	$C_{15}H_{15}O_6^+$	291	-	244	-	-	-	+	-	-	Flavonoid
2	1.532	Caffeic acid hexoside	$C_{15}H_{17}O_9^-$		341	179	-	+	-	-	-	-	Phenolic
3	1.770	Isocitric acid	$C_6H_7O_7^-$	-	191	166	-	-	+	-	-	+	Organic acid
4	3.183	Sinapic acid	$C_{11}H_{12}O_5^+$	225	-	169/154	+	-	-	-	-	-	Phenolic
5	3.507	Salvialinic acid (danshensu)	$C_{26}H_{21}O_{10}^-$	-	197	179	-	-	-	+	-	-	Phenolic
6	4.681	Carnosic acid		333	-	302/225	+	-	-	-	-	-	Diterpene
7	4.868	Isorhamnetin	$C_{16}H_{11}O_7^-$	-	315	163	+	-	-	-	-	-	Flavonoid
8	5.686	7-epi-hydroxyjasmonic acid glucoside	$C_{18}H_{28}O_9^-$	-	387	207	+	+	+	+	+	-	Organic acid
9	6.066	Isorhamnetin 3-(2''-acetylglucoside)	$C_{24}H_{23}O_{13}^-$	-	519	315	-	-	+	-	-	-	Flavonoid
10	6.196	Caffeic acid	$C_9H_7O_4^-$	-	179	151	-	-	-	+	-	-	Phenolic acid
11	6.605	Kaemperfol	$C_{15}H_9O_6^-$	-	285	153	-	-	+	-	-	-	Flavnoid
12	7.405	Luteolin-7-*O* glucuronide	$C_{21}H_{19}O_{12}^+$	463	-	287	+	-	-	-	-	-	Flavonoid
13	7.422	Luteolin -5-glucuronide	$C_{21}H_{17}O_{12}^-$	-	461	327	+	+	-	-	-	-	Flavonoid
14	7.950	Apignin-7-O -glucuronide	$C_{21}H_{19}O_{11}^+$	447	445	219($^+$), 270($^-$)	+	+	-	-	-	-	Flavonoid
15	7.96	Rosmarinic acid	$C_{18}H_{16}O_8^-$	-	359	341	-	-	-	+	+	+	Phenolic acid
16	8.750	Ferulic acid	$C_{10}H_9O_4^-$		193	181/173/ 167/153	-	-	-	-	+	-	Phenolic acid
17	9.482	Quercetin	$C_{15}H_{11}O_7^+$	303	-	286/258	+	-	-	-	+	+	Flavonoid
18	9.635	Trihydroxy-octadecadiendic acid	$C_{18}H_{31}O_5^-$		327	313	-	-	-	-	+	+	Fatty acids
19	9.669	Ellagic acid-di-methyl ether-O-glucoside	$C_{22}H_{19}O_{13}^-$	-	491	401/327	-	-	-	-	-	+	Tannin
20	10.469	Isothymusin	$C_{17}H_{15}O_7^+$	331	-	298	+	-	+	-	-	+	Flavonoid
21	10.513	Cirsiliol	$C_{17}H_{15}O_7^+$	331	-	286	+	-	-	-	-	-	Flavonoid
22	11.508	Dihydroxy dimethoxyflavone	$C_{17}H_{13}O_6^-$	-	313	298	+	-	+	+	+	+	Flavonoid
23	11.525	Cirsimaritin	$C_{17}H_{15}O_6^+$	315	-	279	-	-	+	-	-	+	Flavonoid
24	11.763	Nevadensin	$C_{18}H_{17}O_7^+$	345	-	229/177	+	+	-	+	+	+	Flavonoid
25	14.18	Salvigenin		329	-	282	-	-	-	+	+	+	Flavonoid
26	14.878	4-Sinapoyl-*O*- caffeoyl quinic acid	$C_{27}H_{27}O_{13}^-$	-	559	381	-	-	-	+	-	+	Phenolic acid
27	14.963	Gardenin B	$C_{19}H_{17}O_7^+$	359	-	302/224	-	-	-	-	+	+	Flavonoid
28	15.219	Feruloyl tartaric acid	$C_{14}H_{13}O_9^-$	-	325	310/287	+	+	+	+	-	-	Phenolic acid
29	15.304	Apigenin-*O*-dimethyl ether	$C_{17}H_{15}O_5^+$	299	-	241	-		-	-	-	+	Flavonoid
30	17.159	Caftaric acid	$C_{13}H_{11}O_9^-$	-	311	295/250	+	+	+	-	+	-	Phenolic acid

Note: 1 stands for *O. tenuiflorum* (green variety), 2 for *O. tenuiflorum* (purple variety), 3 for *O. gratissimum*, 4 for *O. basilicum*, 5 for *O. kilimandscharicum* and 6 for *O. americanum*.

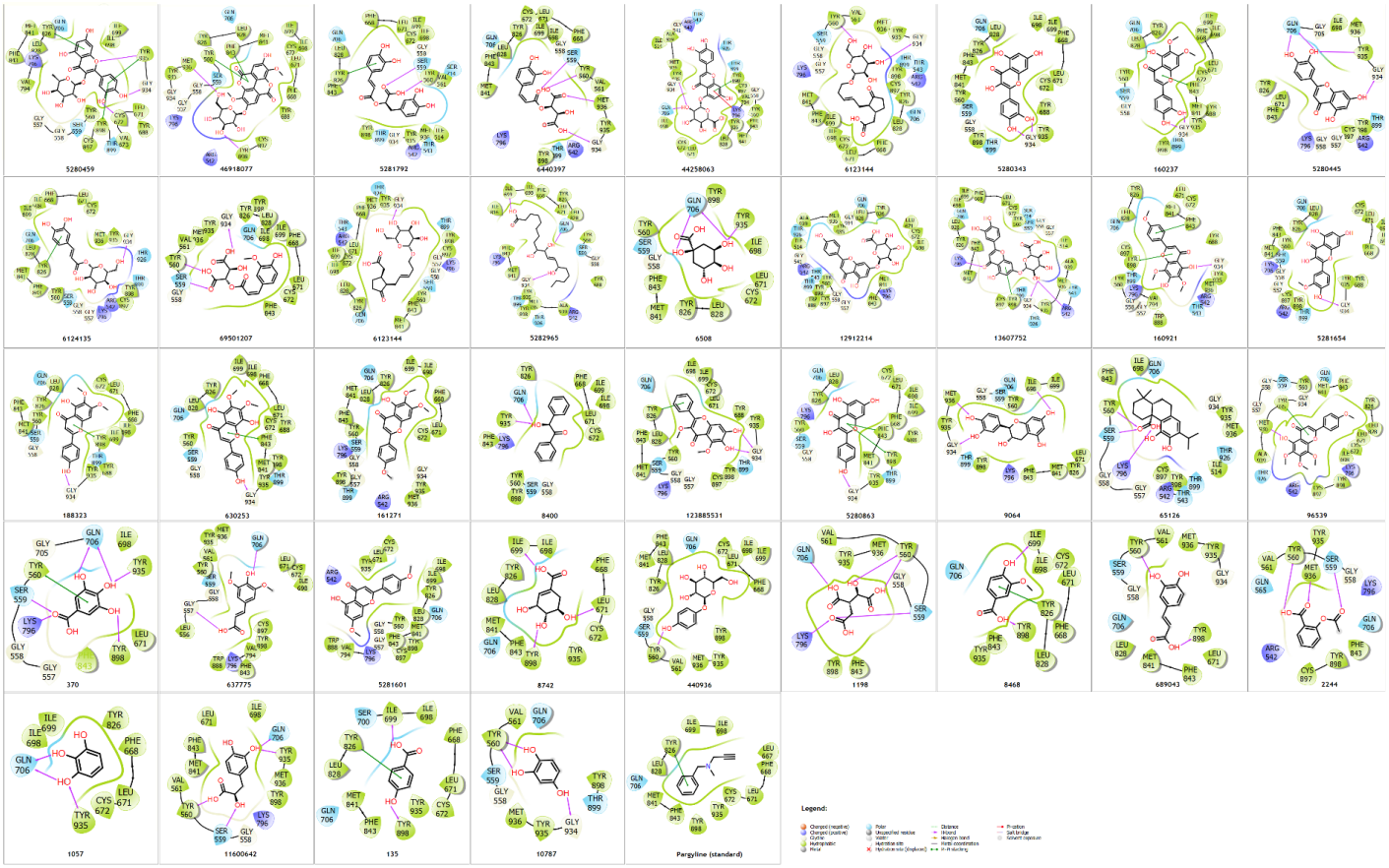

Figure 5: Interactions of the hits from *Ocimum* sp. and the standard inhibitor, pargyline, with the binding site of MAO-B.

inhibitors. The molHERG scores of all the compounds from *Ocimum* sp. were less than 0.5, indicating that none of the compounds are potential HERG inhibitors. In ICM-Pro, mol LD_{50} values <5 mg/kg indicate high toxicity. The IC_{50} values of all the compounds were much higher than 5 mg/kg, indicating that the compounds were not potentially toxic. Compounds with molPAINS scores >0.5 have high probability of being PAINS compounds. The results of ADMET prediction revealed that most of the compounds of *Ocimum* sp. had a high probability of being PAINS compounds (Supplementary Table 1). The molPAMPA scores indicate PAMPA permeability, and scores <-5.0 indicate high permeability. Most of the compounds of *Ocimum* sp. were predicted to have high permeability, as indicated by the molPAMPA scores. The molPGPINHIB and molPGPSUBST scores indicate P-glycoprotein (P-gp) inhibition and P-gp substrate probability, respectively, and scores >0.5 indicate high probability of being P-gp inhibitors or substrates, respectively. The results of ADMET prediction revealed that none of the compounds were P-gp inhibitors or P-gp substrates. The ToxScore provides a measure of chemical toxicity alert, and scores >1 indicate the presence of unfavourable substructures or substituents. Most of the compounds of *Ocimum* sp. contained unfavourable groups, as indicated by the ToxScore. The unfavourable substituents or substructures in the compounds are mentioned in Supplementary Table 1. Ellagic acid-di-methyl ether-O-glucoside, rosmarinic acid, and luteolin-5-glucuronide were identified as top scoring hits against both AChE and MAO-B from molecular docking studies.

DISCUSSION

Oxidative stress resulted from accumulation of reactive oxygen species is a reason for neurodegenerative disorders like Parkinson's disease.[33] Parkinson's disease is the second common neurodegenerative disease. MAO-B inhibitors, AChE inhibitors and L-DOPA are used for the treatment of this disease. Activation of MAO-B is responsible for cognitive dysfunction, destruction of cholinergic neurons, formation of amyloid plaques and catabolism of dopamine. MAO-B inhibitors increase availability of dopamine in the brain by preventing such catabolism.[1,2] Dementia and imbalance in PD patients are treated by AChE inhibitors.[3] However, such treatments have side effects.[5,6] Researchers are trying to find new phytochemicals or food supplements for better treatment options.[34] *In vitro* and *in silico* studies of several phytoconstituents have been studied.[35-40] In traditional Ayurvedic system of medicine *Mucuna pruriens* and *Withania somnifera* have been used to manage neurodegenerative diseases. Other plant of similar relevance is *Curcuma longa*.[41] The present *in vitro* studies showed that the extracts of the leaves of five Indian *Ocimum* species inhibited MAO-B and AChE enzymes. All the species also contained L-DOPA. Compared to

Table 3: Docking scores of the hits from *Ocimum* sp. identified against AChE and MAO-B by docking-based screening.

Receptor	Compound	Glide XP score	Ligand efficiency
AChE	Ellagic acid-di-methyl ether-O-glucoside	-12.154	-0.347
	Luteolin-7-O-glucuronide	-11.957	-0.362
	Rosmarinic acid	-11.581	-0.445
	Luteolin-5-glucuronide	-10.831	-0.328
	7-Epi-12-hydroxyjasmonic acid glucoside	-10.573	-0.392
	Isorhamnetin 3-(2''-acetylglucoside)	-10.136	-0.274
	Quercitrin	-9.785	-0.306
	Catechin	-9.658	-0.460
	Quercetin	-9.640	-0.438
	Caftaric acid	-9.548	-0.434
	Danshensu	-9.497	-0.678
	Apigenin-7,4'-dimethyl ether	-9.372	-0.426
	Isorhamnetin	-9.198	-0.400
	Cirsiliol	-9.093	-0.379
	Apigenin-7-O-glucuronide	-9.093	-0.284
	Feruloyltartaric acid	-8.866	-0.385
	Kaempferol	-8.853	-0.422
	Luteolin	-8.835	-0.421
	Cirsimaritin	-8.727	-0.379
	9,10,13-Trihydroxy-11-octadecenoic acid	-8.363	-0.364
	Salvigenin	-8.351	-0.348
	Gardenin B	-8.327	-0.320
	Dihydroxy dimethoxyflavone	-8.193	-0.356
	Nevadensin	-8.113	-0.325
	Caffeic acid hexoside	-8.026	-0.334
	Isothymusin	-7.527	-0.314
	Caffeic acid	-7.317	-0.563
	Galantamine (standard)	-6.925	-0.330
MAO-B	Quercitrin	-11.948	-0.373
	Ellagic acid-di-methyl ether-O-glucoside	-11.865	-0.339
	Rosmarinic acid	-11.854	-0.456
	Caftaric acid	-11.456	-0.521
	Luteolin-5-glucuronide	-10.524	-0.319
	7-Epi-12-hydroxyjasmonic acid glucoside	-10.511	-0.389
	Quercetin	-10.443	-0.475
	Cirsiliol	-10.381	-0.433
	Luteolin	-10.304	-0.491
	Caffeic acid hexoside	-10.139	-0.422
	Feruloyltartaric acid	-10.028	-0.436
	9,10,13-trihydroxy-11-octadecenoic acid	-9.653	-0.420
	Quinic acid	-9.536	-0.734
	Apigenin-7-O-glucuronide	-9.491	-0.297

Receptor	Compound	Glide XP score	Ligand efficiency
	Luteolin-7-O-glucuronide	-9.307	-0.282
	Nevadensin	-9.135	-0.365
	Isorhamnetin	-9.123	-0.397
	Cirsimaritin	-9.012	-0.392
	Isothymusin	-8.999	-0.375
	Salvigenin	-8.989	-0.375
	Dihydroxy dimethoxyflavone	-8.611	-0.374
	Kaempferol	-8.521	-0.406
	Catechin	-8.402	-0.400
	Carnosic acid	-8.345	-0.348
	Gardenin B	-8.334	-0.321
	Gallic acid	-7.934	-0.661
	Sinapic acid	-7.754	-0.485
	Apigenin-7,4'-dimethyl ether	-7.655	-0.348
	Shikimic acid	-7.518	-0.626
	Arbutin	-7.495	-0.394
	Isocitric acid	-7.296	-0.561
	4-hydroxy-3-methoxy benzoic acid	-7.127	-0.594
	Cinnamic acid	-6.693	-0.608
	Caffeic acid	-6.664	-0.513
	O-acetylsalicylic acid	-6.638	-0.511
	Pyrogallol	-6.429	-0.714
	Danshensu	-6.322	-0.452
	4-hydroxybenzoic acid	-6.023	-0.602
	Benzene-1,2,4-triol	-5.779	-0.642
	Pargyline (standard)	-5.586	-0.466

dopamine that does not cross blood brain barrier, L-DOPA is transported to CNS where it gets converted to dopamine. L-Dopa is used clinically to alleviate symptoms of PD being one of the most effective therapies to manage motor symptoms.[42] Whether the administration of *Ocimum* species could present a better source of L-DOPA with less side effects than pure L-DOPA warrants for further *in vivo* experiments. Chemical synthesis of L-DOPA is time consuming, expensive, and generates racemic mixtures of L-DOPA. Consequently, plants as natural source of L-DOPA presents a low-cost approach to derive enantiomerically pure compound.[43] Other plants reported to be enriched in L DOPA include *Mucuna prurience* (L.) DC. and *Vicia faba* L. of Fabaceae. Now we report this metabolite from six species of *Ocimum*. The three most important *Ocimum* species having all the therapeutic properties to control PD symptoms are *O. basilicum, O. americanum,* and *O. tenuiflorum* (green). L-Dopa content, inhibitory properties against MAO-B and AChE are high in these three species compared to others. During the study a large number of metabolites, mainly phenolic metabolites were identified by GC-MS and LC-MS. To identify the bioactive constituents, docking based screening was performed.

Docking-based virtual screening is frequently employed for the rapid screening of large chemical libraries for identifying top scoring hits.[44] The approach can reduce the cost and time of inhibitor discovery by reducing the number of potential hits, and has proved successful in screening phytochemicals against various targets.[45] Molecular dynamics simulations are also frequently employed in computer-aided drug discovery studies for studying the behaviour of protein-ligand complexes and determining the stability of complexes and protein-ligand interactions. Forty-three compounds, mostly phenolics, were identified from the extracts by GC-MS and HPLC-MS. These phytochemicals were then studied to AChE and MAO-B by molecular docking. The RMSD values between the crystal pose and docked pose of the bound inhibitors generated with Glide XP were 1.352 Å and 1.409 Å for AChE and MAO-B, respectively, indicating good correlation between the docked and crystal poses. Twenty-seven phytochemicals were identified as hits against AChE based on

their docking scores better (lower) than the standard galantamine. Thirty-nine phytochemicals showed better docking score than pargyline (Table 3). The identified phytochemicals were not potentially toxic. Most of the chemicals were found to have high permeability. Ellagic acid-di-methyl ether-O-glucoside (detected in *O. americanum)*, rosmarinic acid (detected in *O. basilicum, O. americanum*), and luteolin-5-glucuronide (detected in the green variety of *O. tenuiflorum)* were identified as top scoring hits against both AChE and MAO-B from molecular docking studies.

CONCLUSION

Out of several therapeutic methods to alleviate symptoms of debilitating neurodegenerative disease PD, three important treatment options are: uses of MAO-B inhibitors, AChE inhibitors, administration of L-DOPA to increase the level of dopamine in the brain. From the above experimental results one important finding is that all the plants contained L-DOPA. The most three important plants are *O. americanum, O. basilicum*, and *O. tenuiflorum* (green). Second important finding is that all the *Ocimum* species inhibited MAO-B. The two most important plants were *O. tenuiflorum* (green) and *O. basilicum*. MAO-B inhibitors are used either alone or in combination with L-DOPA. These two properties are present in *O. tenuiflorum* (green) and *O. basilicum*. Thirdly the *Ocimum* species also inhibited AChE. The three most important plants in this regard are *O. basilicum, O. americanum,* and *O. tenuiflorum* (green). So, the three *Ocimum* species contain all the therapeutic properties to alleviate PD symptoms. Further, ADMET screening indicated that none of the phenolic compounds identified from different *Ocimum* species are potentially toxic. Rosmarinic acid, ellagic acid-di-methyl ether-O-glucoside, and luteolin-5-glucuronide, exhibited strong binding affinity to MAO-B as well as AChE, as indicated by the docking scores. So, it can be concluded that the three *Ocimum* species *O. tenuiflorum* (green), *O. basilicum,* and *O. americanum* have potential value to develop as a natural product nutraceutical for alleviating the PD symptoms without side effects, subject to further *in vivo* experiments.

ACKNOWLEDGEMENT

The research was funded by Department of Science and Technology (Government of West Bengal), University Grants Commission (Centre of advanced studies programme), Department of Science and Technology (FIST programme of Government of India for instrumental facilities).

CONFLICT OF INTEREST

The authors declare that there is no conflict of interests.

REFERENCES

1. Ellis JM, Fell MJ. Current approaches to the treatment of Parkinson's disease. Bioorg Med Chem Lett. 2017; 27(18): 4247-55. doi: 10.1016/j.bmcl.2017.07.075, PMID 28869077.
2. Cai Z. Monoamine oxidase inhibitors: promising therapeutic agents for Alzheimer's disease (Review). Mol Med Rep. 2014; 9(5): 1533-41. doi: 10.3892/mmr.2014.2040, PMID 24626484.
3. Chen JH, Huang TW, Hong CT. Cholinesterase inhibitors for gait, balance, and fall in Parkinson disease: a meta-analysis. npj Parkinsons Dis. 2021; 7(1): 103. doi: 10.1038/s41531-021-00251-1, PMID 34824258.
4. Youdim MBH, Bakhle YS. Monoamine oxidase: isoforms and inhibitors in Parkinson's disease and depressive illness. Br J Pharmacol. 2006; 147;Suppl 1:S287-96. doi: 10.1038/sj.bjp.0706464, PMID 16402116.
5. Finberg JPM, Rabey JM. Inhibitors of MAO-A and MAO-B in psychiatry and neurology. Front Pharmacol. 2016; 7: 340. doi: 10.3389/fphar.2016.00340, PMID 27803666.
6. Seyed MA, Ayesha S, Azmi N, Al-Rabae FM, Al-Alawy AI, Al-Zahrani OR, *et al*. The neuroprotective attribution of *Ocimum basilicum*: a review on the prevention and management of neurodegenerative disorders. Futur J Pharm Sci. 2021; 7(1): 139. doi: 10.1186/s43094-021-00295-3.
7. Gurav TP, Dholakia BB, Giri AP. A glance at the chemodiversity of *Ocimum* species: trends, implications, and strategies for the quality and yield improvement of essential oil. Phytochem Rev. 2022; 21(3): 879-913. doi: 10.1007/s11101-021-09767-z , PMID 34366748.
8. Pattanayak P, Behera P, Das D, Panda SK. *Ocimum sanctum* Linn. A reservoir plant for therapeutic applications: an overview. Pharmacogn Rev. 2010; 4(7): 95. doi: 10.4103/0973-7847.65323.
9. Sultana B, Anwar F, Ashraf M. Effect of extraction solvent/technique on the antioxidant activity of selected medicinal plant extracts. Molecules. 2009; 14(6): 2167-80. doi: 10.3390/molecules14062167, PMID 19553890.
10. Cloete SJ, N'Da CI, Legoabe LJ, Petzer A, Petzer JP. The evaluation of 1-tetralone and 4-chromanone derivatives as inhibitors of monoamine oxidase. Mol Divers. 2021; 25(1): 491-507. doi: 10.1007/s11030-020-10143-w, PMID 32970293.
11. Ellman GL, Courtney KD, Andres V, Featherstone RM. A new and rapid colorimetric determination of acetylcholinesterase activity. Biochem Pharmacol. 1961; 7(2): 88-95. doi: 10.1016/0006-2952(61)90145-9.
12. Farag MA, Ezzat SM, Salama MM, Tadros MG. Anti-acetylcholinesterase potential and metabolome classification of 4 *Ocimum* species as determined via UPLC/qTOF/MS and chemometric tools. J Pharm Biomed Anal. 2016; 125: 292-302. doi: 10.1016/j.jpba.2016.03.037, PMID 27061877.
13. Kind T, Wohlgemuth G, Lee DY, Lu Y, Palazoglu M, Shahbaz S, *et al*. FiehnLib: mass spectral and retention index libraries for metabolomics based on quadrupole and time-of-flight gas chromatography/mass spectrometry. Anal Chem. 2009; 81(24): 10038-48. doi: 10.1021/ac9019522, PMID 19928838.
14. Das S, Dutta M, Chaudhury K, De B. Metabolomic and chemometric study of *Achras sapota* L. fruit extracts for identification of metabolites contributing to the inhibition of α-amylase and α-glucosidase. Eur Food Res Technol. 2016; 242(5): 733-43. doi: 10.1007/s00217-015-2581-0.
15. Sadasivam S, Manikam A. Biochemical methods. India: Wiley Eastern Limited; 1992.
16. Lu C, Wu C, Ghoreishi D, Chen W, Wang L, Damm W, *et al*. OPLS4: improving force field accuracy on challenging regimes of chemical space. J Chem Theor Comput. 2021; 17(7): 4291-300. doi: 10.1021/acs.jctc.1c00302, PMID 34096718.
17. Berman HM, Westbrook J, Feng Z, Gilliland G, Bhat TN, Weissig H, *et al*. The Protein Data Bank. Nucleic Acids Res. 2000; 28(1): 235-42. doi: 10.1093/nar/28.1.235, PMID 10592235.
18. Binda C, Newton-Vinson P, Hubálek F, Edmondson DE, Mattevi A. Structure of human monoamine oxidase B, a drug target for the treatment of neurological disorders. Nat Struct Biol. 2002; 9(1): 22-6. doi: 10.1038/nsb732, PMID 11753429.
19. Cheung J, Rudolph MJ, Burshteyn F, Cassidy MS, Gary EN, Love J, *et al*. Structures of human acetylcholinesterase in complex with pharmacologically important ligands. J Med Chem. 2012; 55(22): 10282-6. doi: 10.1021/jm300871x, PMID 23035744.
20. Webb B, Sali A. Comparative protein structure modeling using MODELLER. Curr Protoc Bioinformatics. 2014; 5.6.1-5.6.32;47(1). doi: 10.1002/0471250953.bi0506s47.
21. Sastry GM, Adzhigirey M, Day T, Annabhimoju R, Sherman W. Protein and ligand preparation: parameters, protocols, and influence on virtual screening enrichments. J Comput Aid Mol Des. 2013; 27(3): 221-34. doi: 10.1007/s10822-013-9644-8, PMID 23579614.
22. Olsson MHM, Søndergaard CR, Rostkowski M, Jensen JH. PROPKA3: consistent treatment of internal and surface residues in empirical p K a predictions. J Chem Theor Comput. 2011; 7(2): 525-37. doi: 10.1021/ct100578z, PMID 26596171.
23. Søndergaard CR, Olsson MHM, Rostkowski M, Jensen JH. Improved treatment of ligands and coupling effects in empirical calculation and rationalization of p K a values. J Chem Theor Comput. 2011; 7(7): 2284-95. doi: 10.1021/ct200133y, PMID 26606496.
24. Friesner RA, Murphy RB, Repasky MP, Frye LL, Greenwood JR, Halgren TA, *et al*. Extra precision glide: docking and scoring incorporating a model of hydrophobic enclosure for protein ligad complexex. J Med Chem. 2006; 49(21): 6177-96. doi: 10.1021/jm051256o, PMID 17034125.
25. Halgren TA, Murphy RB, Friesner RA, Beard HS, Frye LL, Pollard WT, *et al*. Glide: A new approach for rapid, accurate docking and scoring. 2. Enrichment factors in database screening. J Med Chem. 2004; 47(7): 1750-9. doi: 10.1021/jm030644s, PMID 15027866.
26. Maestro Release 2021-2; Schrödinger, 2021 (No. 2021-2).

27. Tripathi AC, Upadhyay S, Paliwal S, Saraf SK. Privileged scaffolds as MAO inhibitors: retrospects and prospects. Eur J Med Chem. 2018; 145: 445-97. doi: 10.1016/j.ejmech.2018.01.003, PMID 29335210.
28. Debnath M, Das S, Bhowmick S, Karak S, Saha A, De B. Anti-Alzheimer's potential of different varieties of *Piper betle* leaves and molecular docking analysis of metabolites. Free Radic Antioxid. 2021; 11(1): 13-8. doi: 10.5530/fra.2021.1.3.
29. Sarkar S, Ul Hoda M, Das S. Anti-melanogenic, antioxidant potentialities and metabolome classification of six *Ocimum* species: metabolomics and *in silico* approaches. Trends Phytochem Res. 2023; 7(1): 30-50.
30. Abdel Shakour ZT, El-Akad RH, Elshamy AI, El Gendy AEG, Wessjohann LA, Farag MA. Dissection of *Moringa oleifera* leaf metabolome in context of its different extracts, origin and in relationship to its biological effects as analysed using molecular networking and chemometrics. Food Chem. 2023; 399: 133948. doi: 10.1016/j.foodchem.2022.133948, PMID 35994855.
31. Chen Y, Yu H, Wu H, Pan Y, Wang K, Jin Y, *et al*. Characterization and quantification by LC-MS/MS of the chemical components of the heating products of the flavonoids extract in pollen *Typhae* for transformation rule exploration. Molecules. 2015; 20(10): 18352-66. doi: 10.3390/molecules201018352, PMID 26457703.
32. Pandey R, Kumar B. HPLC-QTOF-MS/MS-based rapid screening of phenolics and triterpenic acids in leaf extracts of *Ocimum* species and their interspecies variation. J Liq Chromatogr Relat Technol. 2016; 39(4): 225-38. doi: 10.1080/10826076.2016.1148048.
33. Olufunmilayo EO, Gerke-Duncan MB, Holsinger RMD. Oxidative stress and antioxidants in neurodegenerative disorders. Antioxidants (Basel). 2023; 12(2): 517. doi: 10.3390/antiox12020517, PMID 36830075.
34. Kumar A, P N, Kumar M, Jose A, Tomer V, Oz E, *et al*. Major phytochemicals: recent advances in health benefits and extraction method. Molecules. 2023; 28(2): 887. doi: 10.3390/molecules28020887, PMID 36677944.
35. Vijayakumar S, Prabhu S, Rajalakhsmi S, Manogar P. Review of potential phytocompounds in drug development for Parkinson disease: A pharmacoinformatic approach. Inform Med Unlocked. 2016; 5: 15-25. doi: 10.1016/j.imu.2016.09.002.
36. Shahpiri Z, Bahramsoltani R, Hosein Farzaei M, Farzaei F, Rahimi R. Phytochemicals as future drugs for Parkinson's disease: a comprehensive review. Rev Neurosci. 2016; 27(6): 651-68. doi: 10.1515/revneuro-2016-0004, PMID 27124673.
37. Anastácio JR, Netto CA, Castro CC, Sanches EF, Ferreira DC, Noschang C, *et al*. Resveratrol treatment has neuroprotective effects and prevents cognitive impairment after chronic cerebral hypoperfusion. Neurol Res. 2014; 36(7): 627-33. doi: 10.1179/1743132813Y.0000000293, PMID 24620966.
38. Lee H, Kim YO, Kim H, Kim SY, Noh HS, Kang SS, *et al*. Flavonoid wogonin from medicinal herb is neuroprotective by inhibiting inflammatory activation of microglia. FASEB J. 2003; 17(13): 1943-4. doi: 10.1096/fj.03-0057fje, PMID 12897065.
39. Sandoval-Avila S, Diaz NF, Gómez-Pinedo U, Canales-Aguirre AA, Gutiérrez-Mercado YK, Padilla-Camberos E, *et al*. Neuroprotective effects of phytochemicals on dopaminergic neuron cultures. Neurologia (Engl Ed). 2019; 34(2): 114-24. doi: 10.1016/j.nrl.2016.04.018, PMID 27342389.
40. Rahman MM, Wang X, Islam MR, Akash S, Supti FA, Mitu MI, *et al*. Multifunctional role of natural products for the treatment of Parkinson's disease: at a glance. Front Pharmacol. 2022; 13: 976385. doi: 10.3389/fphar.2022.976385, PMID 36299886.
41. Pathak-Gandhi N. Vaidya ADV. Management of Parkinson's disease in Ayurveda: medicinal plants and adjuvant measures. J Ethnopharmacol. 2017; 197: 56-1.
42. Muthuraman M, Koirala N, Ciolac D, Pintea B, Glaser M, Groppa S, *et al*. Deep brain stimulation and L-dopa therapy: concepts and action in Parkinson's disease. Front Neurol. 2018; 9: 711. doi: 10.3389/fneur.2018.00711, PMID 30210436.
43. Tesoro C, Lelario F, Ciriello R, Bianco G, Di Capua A, Acquavia MA. An overview of methods for L-dopa extraction and analytical determination in plant matrices. Separations. 2022; 9(8): 224. doi: 10.3390/separations9080224.
44. Kapetanovic IM. Computer-aided drug discovery and development (CADDD): *in silico*-chemico-biological approach. Chem Biol Interact. 2008; 171(2): 165-76. doi: 10.1016/j.cbi.2006.12.006, PMID 17229415.
45. Ma DL, Chan DSH, Leung CH. Molecular docking for virtual screening of natural product databases. Chem Sci. 2011; 2(9): 1656-65. doi: 10.1039/C1SC00152C.

Cite this article: Sarkar S, Chatterjee J, Gangopadhyay A, Sheashea M, Farag MA, Saha A, *et al*. Anti-Parkinson Potential of Indian *Ocimum* species in Relation to Active Components as Revealed Using Metabolites Profiling, *in vitro* and *in silico* Enzyme Inhibition Studies. Free Radicals and Antioxidants. 2023;13(2):74-85.

Supplementary Table 1: ADMET properties of the compounds of *Ocimum.* sp.

PubChem ID/ Chemical name	Lipinski's rule of five				Veber's rules		BBB score	CACO2	Plasma half-life (hours)	molHERG score	LD_{50} (mg/kg)	molPAINS	molPAMPA	molPGPINHIB	molPGPSUBST	Names of unfavourable groups	ToxScore
	MW (Da)	logP	HBA	HBD	TPSA (Å²)	Rot. bonds											
6124135	342.0951	-3.9253	10	6	126.23	5	1.76302	-5.6506	3.564854	0.2334	111.809	0.387032	-5.49012	0.036718	0.14719	Michael acceptor;Para-hydroxysubstituted methyl phenyl ether; quinone-like	2.281831
8468	168.0423	-1.4399	5	2	52.825	2	2.86426	-4.85712	1.862137	0.10681	306.322	0.083541	-4.85572	0.14399	0.310574	quinone-like	0.213201
135	138.0317	-0.6273	4	2	46.264	1	2.81603	-4.69385	1.454022	0	287.949	0.053801	-4.94703	0	0.080643	Carboxylic acids	0.5
101522313	560.153	-3.7747	16	6	161.82	11	1.30854	-5.78645	1.811087	0.10681	158.742	0.716241	-5.3411	0.194564	0.402001	Michael acceptor; quinone-like	2.279206
6123144	388.1733	-6.4393	11	5	122.68	9	1.19645	-5.71086	5.39512	0.18211	32.2375	0.323585	-5.71984	0.031542	0.187078	Carboxylic acids	0.5
5282965	330.2406	-4.0888	6	4	77.818	15	2.21774	-4.94103	2.023696	0.18211	75.6519	0.627225	-4.88455	0.047039	0.129601	quinone-like	0.213201
12912214	446.0849	-2.1251	13	6	146.86	4	1.65886	-5.74605	4.271582	0.18211	168.01	0.507513	-5.26123	0.06759	0.192665	Carboxylic acids;resorcinol	0.816228
5281601	298.0841	0.9646	6	1	53.421	3	3.92082	-4.96994	10.063111	0.10681	212.238	0.233292	-4.51763	0.204654	0.29496	resorcinol	0.316228
440936	272.0896	-3.6717	7	5	97.714	3	2.45046	-4.9595	5.354781	0.18211	76.9439	0.028283	-5.26188	0.036718	0.07424	quinone-like	0.447214
10787	126.0317	-0.8264	3	3	50.952	0	2.66537	-4.91357	1.825911	0	138.701	0.353212	-5.17098	0	0.099422	quinone-like; resorcinol	2.13726
8400	212.0837	1.45123	3	1	29.39	3	4.90886	-4.71905	0.426656	0.18211	218.898	0.053801	-4.61671	0.01068	0		0
689043	180.0423	-0.9072	5	3	61.718	2	2.79557	-4.94773	1.09902	0.10681	360.806	0.443767	-5.3123	0	0.117673	Carboxylic acids;Michael acceptor; quinone-like	2.928278
6440397	312.0481	-3.3625	12	5	125.65	7	1.79979	-5.37616	0.779401	0.18211	187.835	0.451723	-5.42076	0.026353	0.158738	Carboxylic acids; Michael acceptor;Para-hydroxysubstituted methyl phenyl ether; quinone-like	2.857305
65126	332.1988	-2.5631	5	3	59.446	2	3.42337	-5.14194	4.250005	0.31051	145.376	0.785097	-4.85976	0.015928	0.111641	Carboxylic acids; quinone-like; resorcinol	1.493156
9064	290.079	-1.8367	6	5	90.448	1	2.73177	-4.96768	6.400748	0.18211	134.667	0.496223	-5.10961	0.031542	0.15298	quinone-like; resorcinol	1.662937
444539	148.0524	1.16351	3	1	28.622	2	4.25872	-4.7334	0.929106	0.18211	235.199	0.009576	-4.64977	0	0	Carboxylic acids; Michael acceptor	1.788675
160237	330.0739	-0.3578	8	3	85.708	3	2.75041	-5.19223	3.240727	0.10681	216.61	0.827685	-4.47338	0.184466	0.376954	quinone-like; resorcinol	1.169032

PubChem ID/ Chemical name	Lipinski's rule of five				Veber's rules		BBB score	CACO2	Plasma half-life (hours)	molHERG score	LD_{50} (mg/kg)	molPAINS	molPAMPA	molPGPINHIB	molPGPSUBST	Names of unfavourable groups	ToxScore
	MW (Da)	logP	HBA	HBD	TPSA ($Å^2$)	Rot. bonds											
188323	314.079	0.38758	7	2	70.229	3	2.98731	-4.83732	4.244399	0.10681	204.362	0.774465	-4.53072	0.189516	0.361805	quinone-like	0.213201
11600642	198.0528	-2.5227	6	4	77.895	3	2.61613	-5.09363	1.029235	0.10681	109.926	0.359878	-5.11189	0.026353	0.135502	Carboxylic acids; quinone-like; resorcinol	1.493156
123885531	314.079	-0.0568	7	2	67.884	3	3.02005	-4.86972	2.785196	0.10681	226.039	0.82547	-4.44491	0.189516	0.371915	Carboxylic acids; quinone-like; resorcinol	1.531305
46918077	492.0904	-4.2154	15	5	153.11	5	1.52306	-6.0593	8.416611	0	147.593	0.677744	-5.37536	0.224813	0.289728	-	0
(+)-Catechin-3-O- β-D-gluco(2, 6-bis-cinnamoyl)-pyranoside	712.2156	0.70104	15	6	160.97	12	0.1994	-6.00999	1.995233	0.10681	92.927	0.671225	-5.59105	0.062462	0.27922	Michael acceptor; quinone-like; resorcinol	2.783707
445858	194.0579	-1.2525	5	2	52.801	3	2.96648	-4.77919	1.451775	0.10681	372.612	0.197816	-5.16413	0.154123	0.300179	Michael acceptor; quinone-like	1.426402
69501207	326.0638	-3.7078	12	4	116.73	8	2.15413	-5.28817	1.106694	0.10681	155.42	0.249407	-5.24944	0.179414	0.33121	Carboxylic acids;Michael acceptor;quinone-like	1.713201
370	170.0215	-1.7237	6	4	77.222	1	2.52365	-4.96303	2.170396	0.10681	162.447	0.555997	-4.98891	0.015928	0.08697	Carboxylic acids;quinone-like; resorcinol	1.706357
96539	358.1053	-0.8044	8	1	67.644	5	2.94833	-4.87496	5.070292	0	269.693	0.564913	-4.47556	0.260029	0.27922	quinone-like; resorcinol	0.779955
1198	192.027	-4.3458	10	4	101.39	5	1.76199	-5.31257	0.477682	0.14956	95.5272	0.118446	-5.27213	0.031542	0.117673	quinone-like	0.213201
44259375	520.1217	-4.703	15	6	163.44	7	1.43336	-5.85117	4.477953	0.2334	90.5275	0.640662	-5.06488	0.204654	0.392011	quinone-like	0.213201
5281654	316.0583	-1.4999	8	4	93.693	2	2.65973	-5.39951	3.120164	0.10681	444.769	0.68585	-4.51081	0.179414	0.387002	quinone-like	0.213201
630253	330.0739	-0.1265	8	3	85.479	3	2.75361	-5.12435	2.538594	0.10681	255.752	0.836515	-4.53282	0.189516	0.376954	Carboxylic acids;quinone-like; resorcinol	1.104903
5280863	286.0477	-0.4501	7	4	87.131	1	2.77807	-5.15602	3.365119	0.20942	410.678	0.525143	-4.5767	0.041883	0.187078	Carboxylic acids	0.5
44258063	462.0798	-2.7405	14	7	163.49	4	1.614	-5.80221	4.100699	0.2334	195.166	0.644	-5.40363	0.06759	0.214777	quinone-like; resorcinol	1.522585
13607752	462.0798	-2.8704	14	7	162.34	4	1.614	-5.80062	3.649769	0.2334	176.616	0.660565	-5.32901	0.06759	0.214777	Carboxylic acids;quinone-like; resorcinol	1.955831
5280445	286.0477	0.69799	7	4	89.047	1	2.75133	-5.08324	4.253094	0.20942	351.904	0.725708	-4.67842	0.041883	0.175826	Michael acceptor;quinone-like	1.141479
160921	344.0896	-0.3582	8	2	75.406	4	2.86908	-4.89088	4.893465	0	259.138	0.823253	-4.53621	0.224813	0.351652	quinone-like; resorcinol	0.976643

PubChem ID/ Chemical name	Lipinski's rule of five				Veber's rules		BBB score	CACO2	Plasma half-life (hours)	molHERG score	LD_{50} (mg/kg)	molPAINS	molPAMPA	molPGPINHIB	molPGPSUBST	Names of unfavourable groups	ToxScore
	MW (Da)	logP	HBA	HBD	TPSA (Å^2)	Rot. bonds											
2244	180.0423	-0.668	6	1	49.484	3	2.96637	-4.846	0.49553	0	654.421	0	-4.68477	0.01068	0.01006	ester or carbamate; quinone-like	1.213201
1057	126.0317	-0.4693	3	3	48.814	0	2.69522	-4.92917	2.074964	0	79.3627	0.524222	-4.85113	0	0.105559	quinone-like; resorcinol	1.706357
5280343	302.0427	-1.1072	8	5	102.61	1	2.55121	-5.21627	2.828291	0.18211	450.179	0.746793	-4.51512	0.041883	0.181465	quinone-like; resorcinol	1.206357
5280459	448.1006	-3.4552	12	7	150.41	3	1.65886	-5.71338	5.268632	0.20942	144.694	0.694714	-4.97017	0.06759	0.225703	quinone-like; resorcinol	1.169032
6508	192.0634	-4.8397	7	5	90.685	1	1.91151	-4.8778	1.830135	0	119.405	0.140272	-5.38256	0.01068	0.08697	Carboxylic acids	0.5
5281792	360.0845	-1.8161	10	5	114.27	7	2.2973	-5.69417	0.53541	0.14956	676.128	0.571997	-5.35827	0.015928	0.175826	Michael acceptor; quinone-like; resorcinol	2.382233
161271	328.0947	0.15597	7	1	60.156	4	3.58225	-4.80646	6.751469	0	208.016	0.538861	-4.4636	0.239915	0.27922	resorcinol	0.353553
8742	174.0528	-3.1613	6	4	75.58	1	2.06693	-4.74543	2.735618	0	37.9156	0.11462	-5.26791	0.02115	0.054472	Carboxylic acids	0.5
637775	224.0685	-1.4828	6	2	59.362	4	2.94221	-4.84352	1.927099	0.14956	245.768	0.465484	-5.0275	0.169304	0.305383	Carboxylic acids; Michael acceptor	1.788675

MW: Molecular weight (≤500, Lipinski's rule of five); logP: Octanol-water Partition coefficient (≤5, Lipinski's rule); HBA: Number of Hydrogen Bond Acceptors (≤10, Lipinski's rule); HBD: Number of Hydrogen Bond Donors (≤5, Lipinski's rule); TPSA: Total Polar Surface Area (≤140, Veber's rule); Rot. Bonds: Number of Rotatable Bonds (≤10, Veber's rule); BBB score: Blood-Brain Barrier permeability (>4 indicates BBB permeability); CACO2: $CACO_2$ cell permeability (>5 indicates high permability); molHERG: predicted HERG inhibition (>0.5 indicates HERG inhibition); LD50: <5 indicates high toxicity; molPAINS: Predicted PAINS probability (>0.5 indicates high PAINS probability); molPAMPA: Predicted PAMPA permeability (>5 indicates high permeability); molGPIINHIB: P-glycoprotein (P-gp) inhibitor probability (>0.5 indicates high probability of being P-gp inhibitor); molPGPSUBST: Probability of being P-gp substrate (>0.5 indicates high P-gp substrate probability); ToxScore: Toxicity score (>1 indicates presence of unfavourable substructures/ substituents). The unfavourable parameters are in red. For molPAMPA, BBB, and CACO-2 permeability, the values in green indicate high permeability.